# Disentangling the hadronic from the leptonic emission in the composite SNR G326.3-1.8

**Justine Devin**
with F. Acero, J. Ballet, J. Schmid

IAUS 331: SN1987A, 30 years later
22th February 2017

# SNR G326.3-1.8

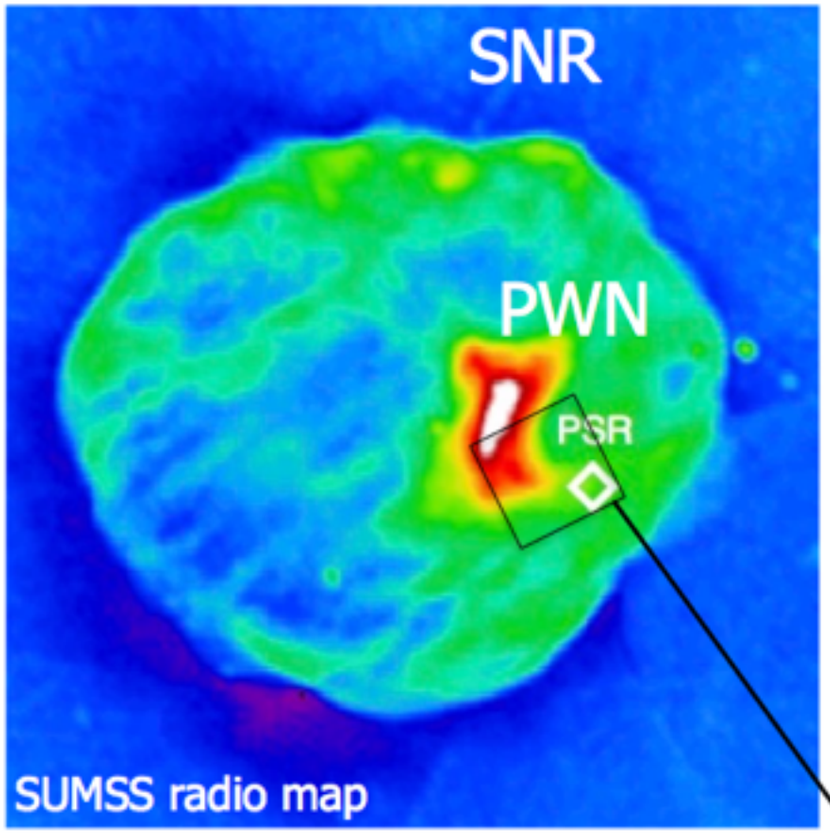


Whiteoak & Green, 96

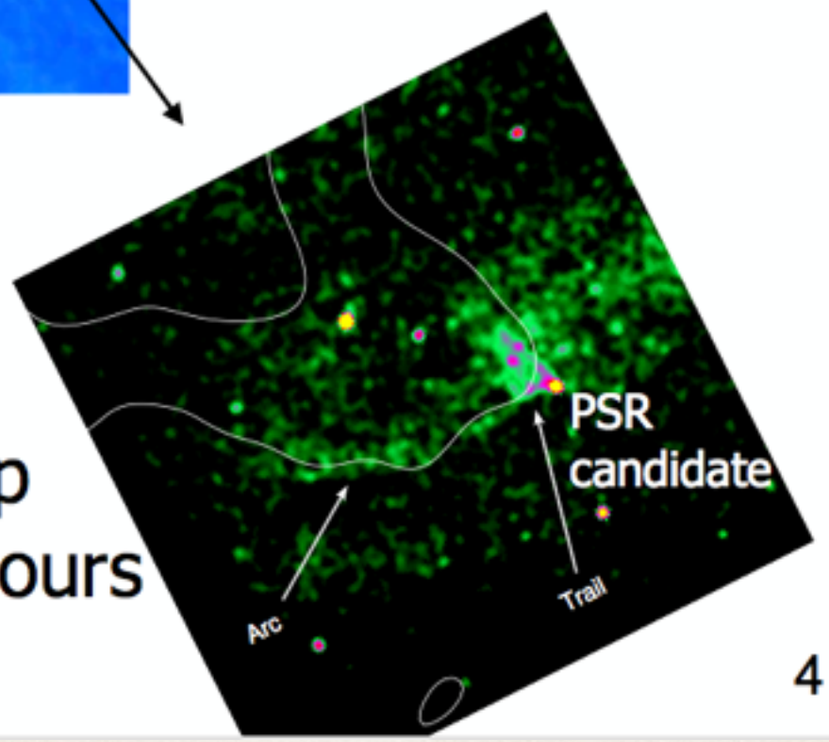


Chandra map
+ radio contours
Temim+13

$$D \approx 4.1 kpc$$

$$v_{pulsar} \approx 410 km.s^{-1}$$

$$v_{shock} \approx 500 km.s^{-1}$$

**16 500 years old,**
**PWN already crushed**
**by the reverse shock**

# Fermi/LAT data - Test Statistic map

**300 MeV - 300 GeV**

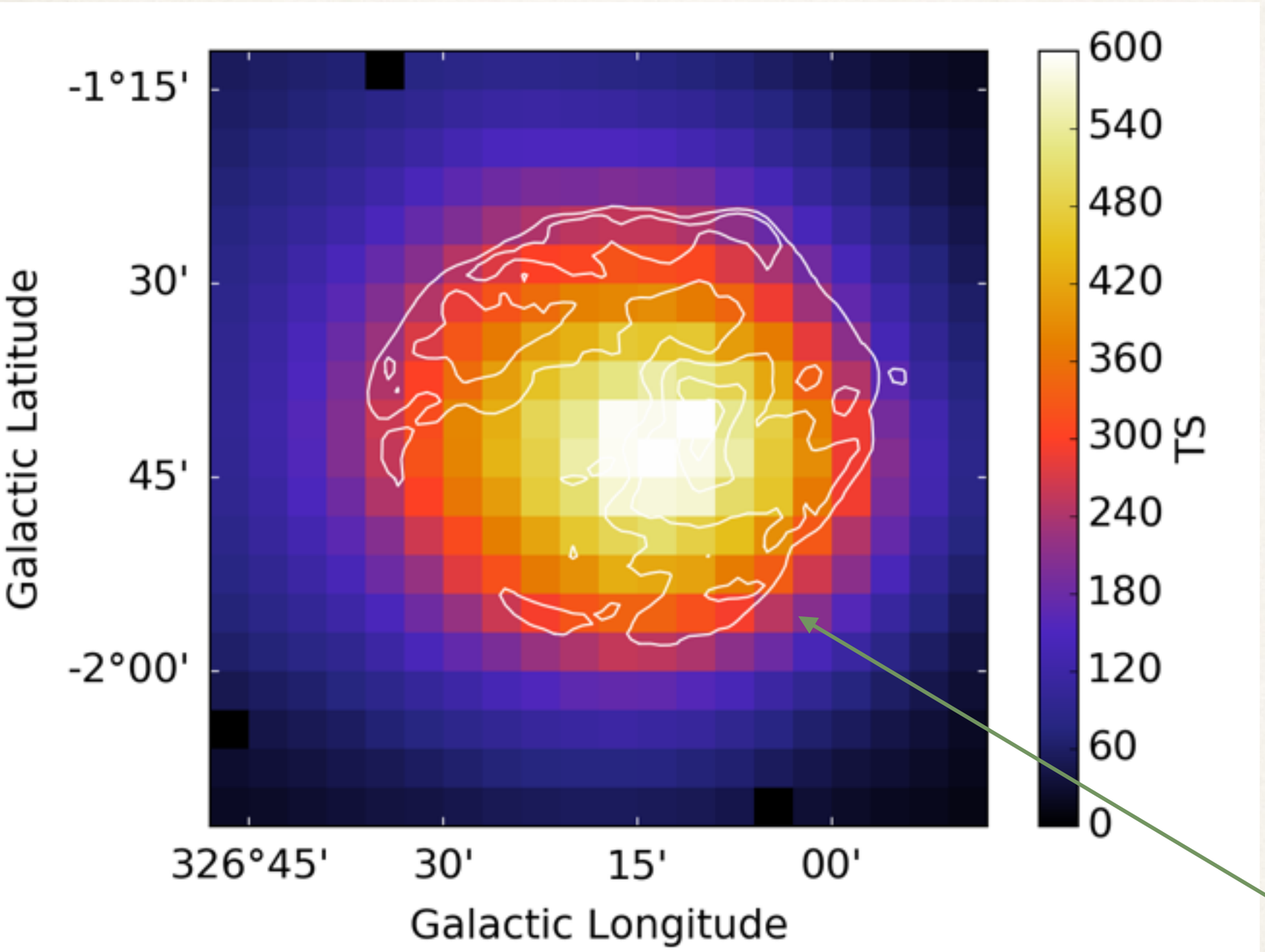


**1. Is emission coming from the shell or the nebula ?**

**2. Hadronic or leptonic origins ?**

**radio contours**

# Energy-dependent morphology

## 2D symmetrical Gaussian fitted in 5 energy bands

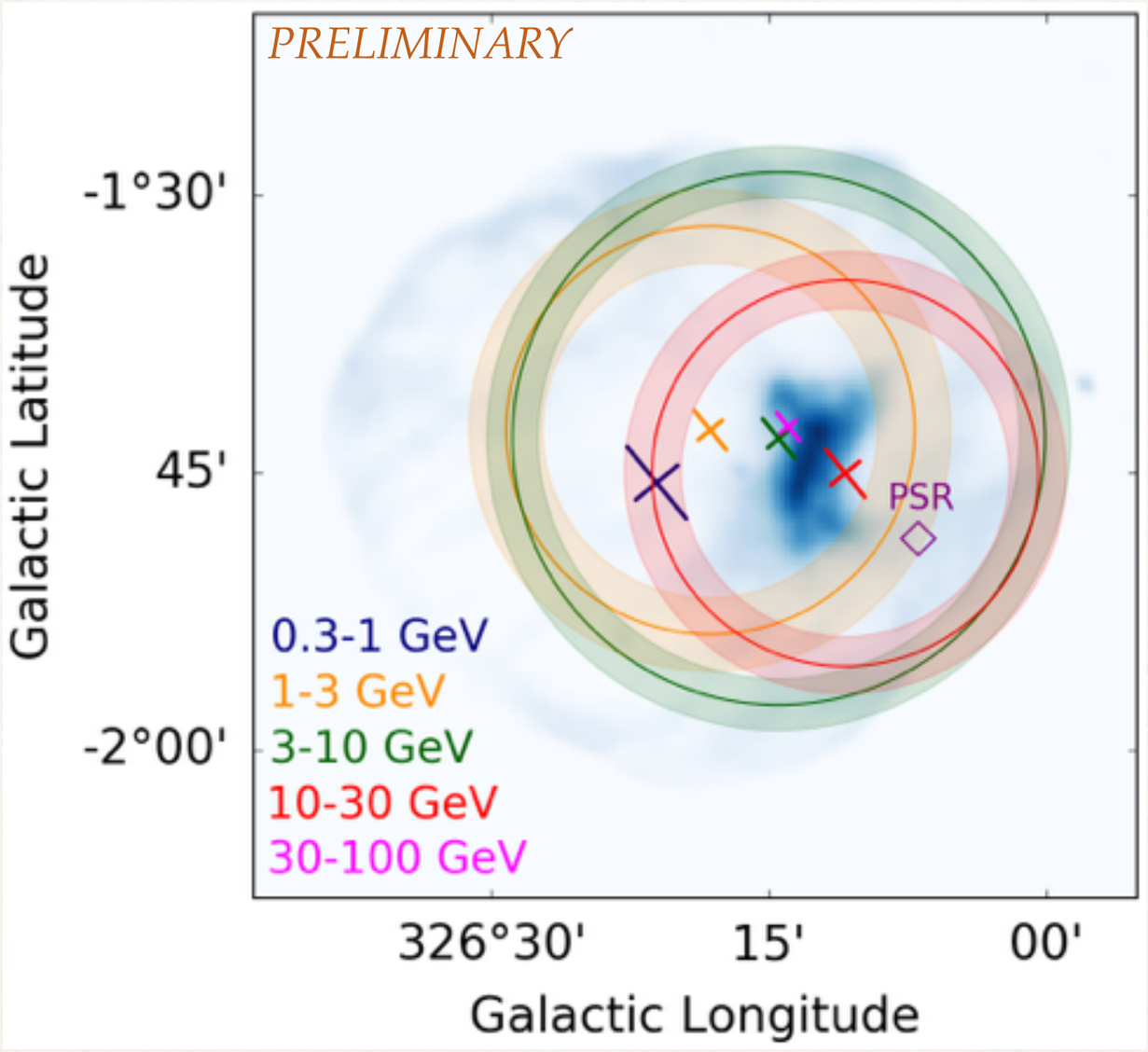


**Emission significantly extended from 1 GeV to 30 GeV**

**=> Clear trend toward the PWN at higher energies**

# Morphological analysis

## Templates:

### radio PWN:

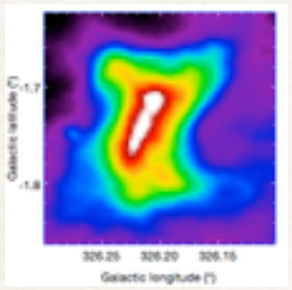


### radio SNR:

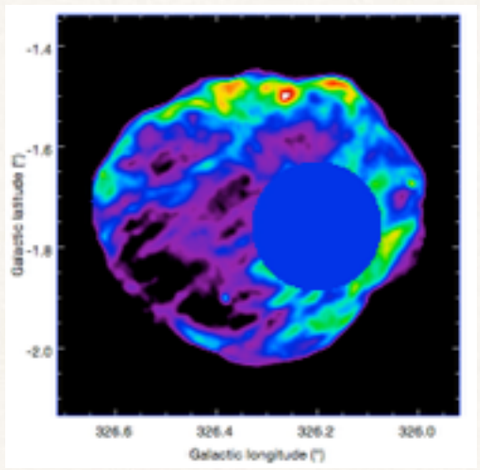


### SNR mask:

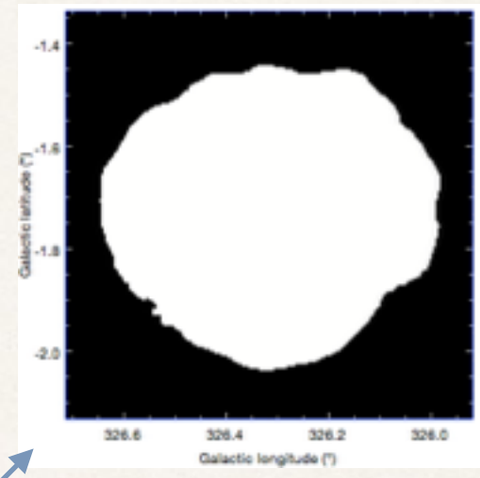


**Best model to reproduce the gamma-ray emission**

# Spectral energy distribution

## SNR mask + radio PWN:

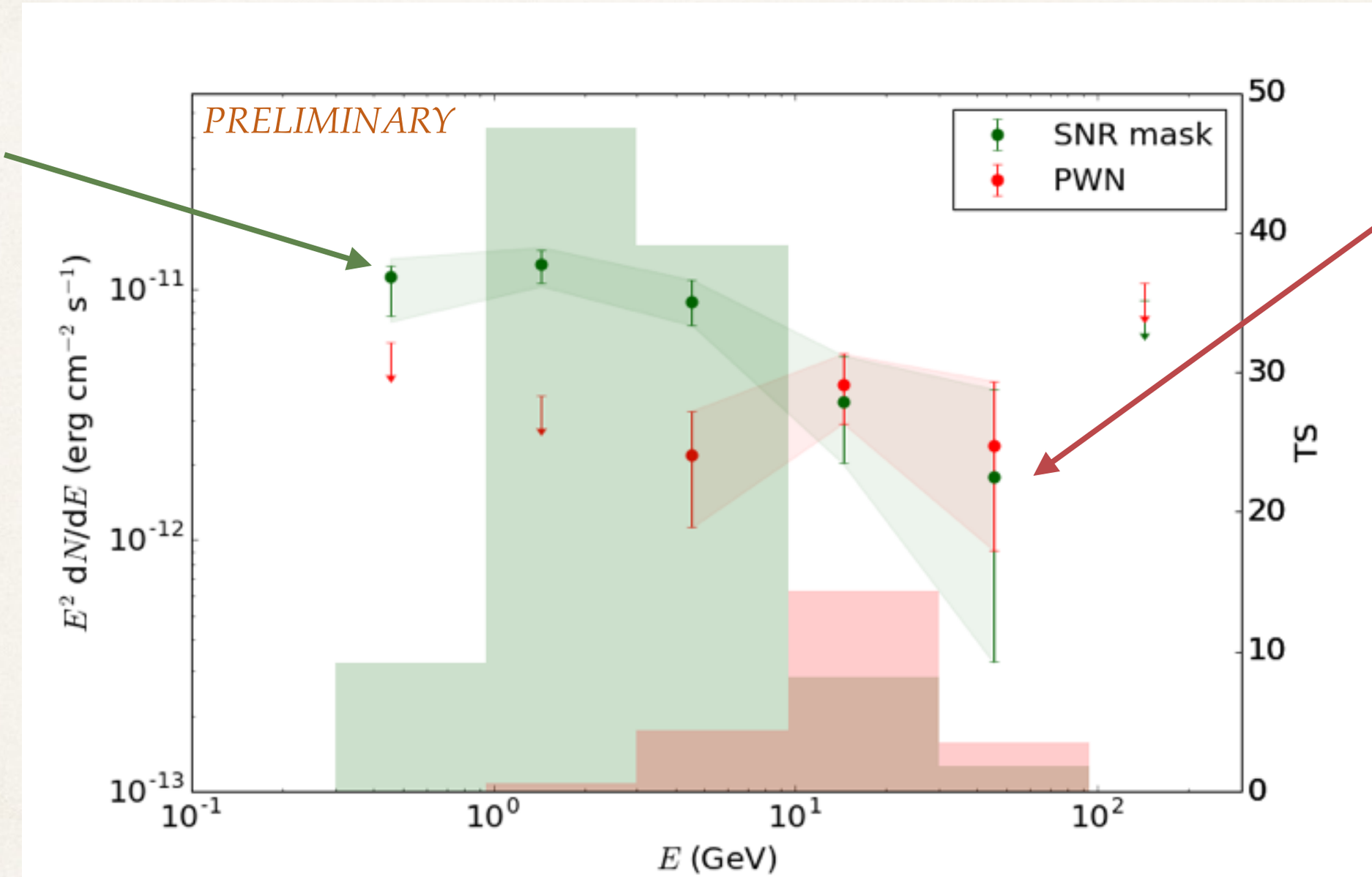


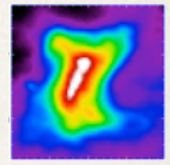

**SNR mask:**

$\Gamma = 2.17 \pm 0.06$

**PWN:**

$\Gamma = 1.79 \pm 0.12$

# Conclusions

## Morphological analysis of SNR G326.3-1.8

* Source is significantly extended
* Energy-dependent morphology shows a clear trend toward the PWN at higher energies

## Spectral analysis of SNR G326.3-1.8

* Spectral energy distribution reveals two different spectral signatures which might suggest different origins (hadronic and leptonic for the SNR and the PWN, respectively)

**Thanks for your attention!**

# BACKUP SLIDES

# Extension of the source

## Best fitted Disk:

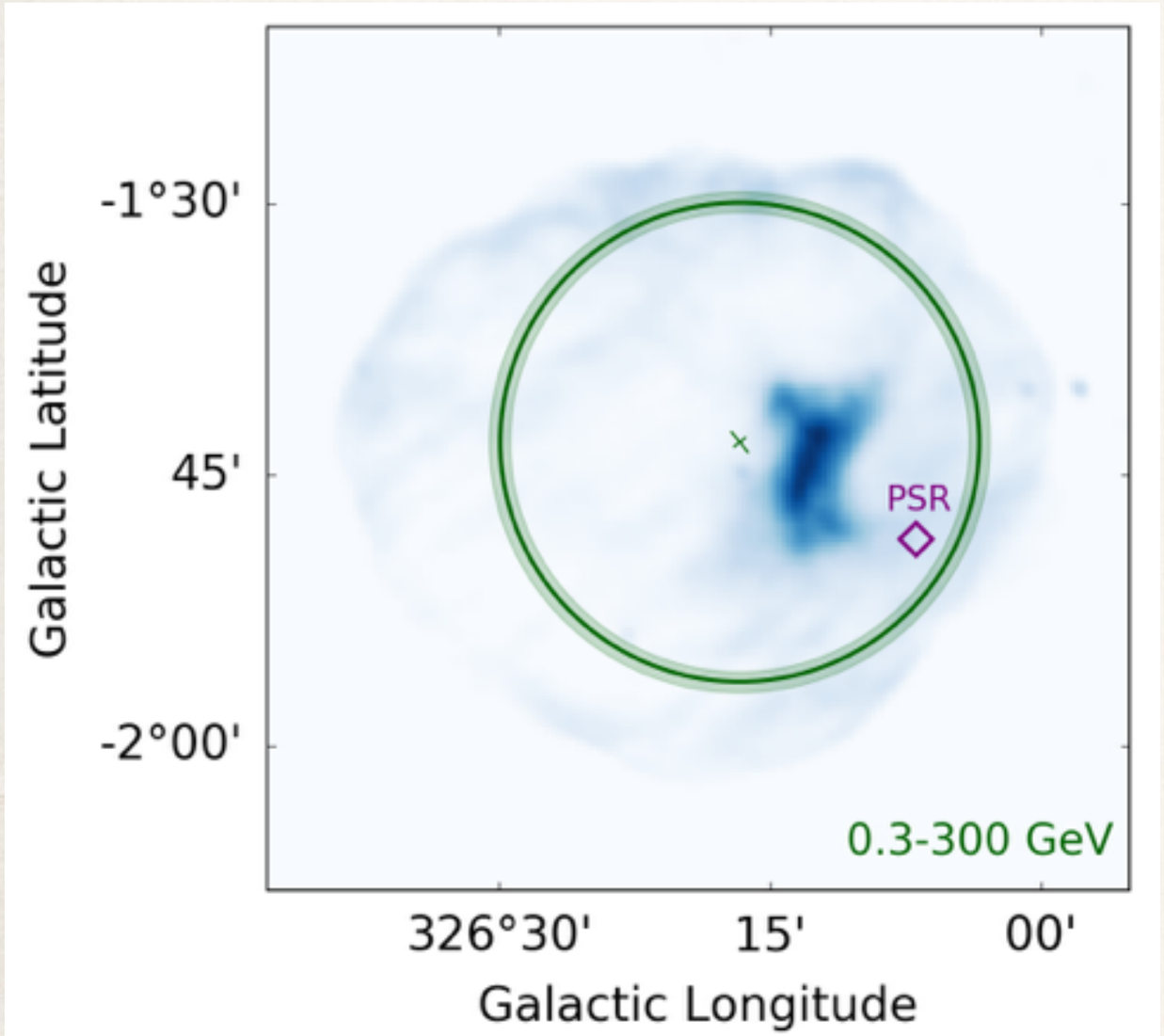


## Best fitted Gaussian:

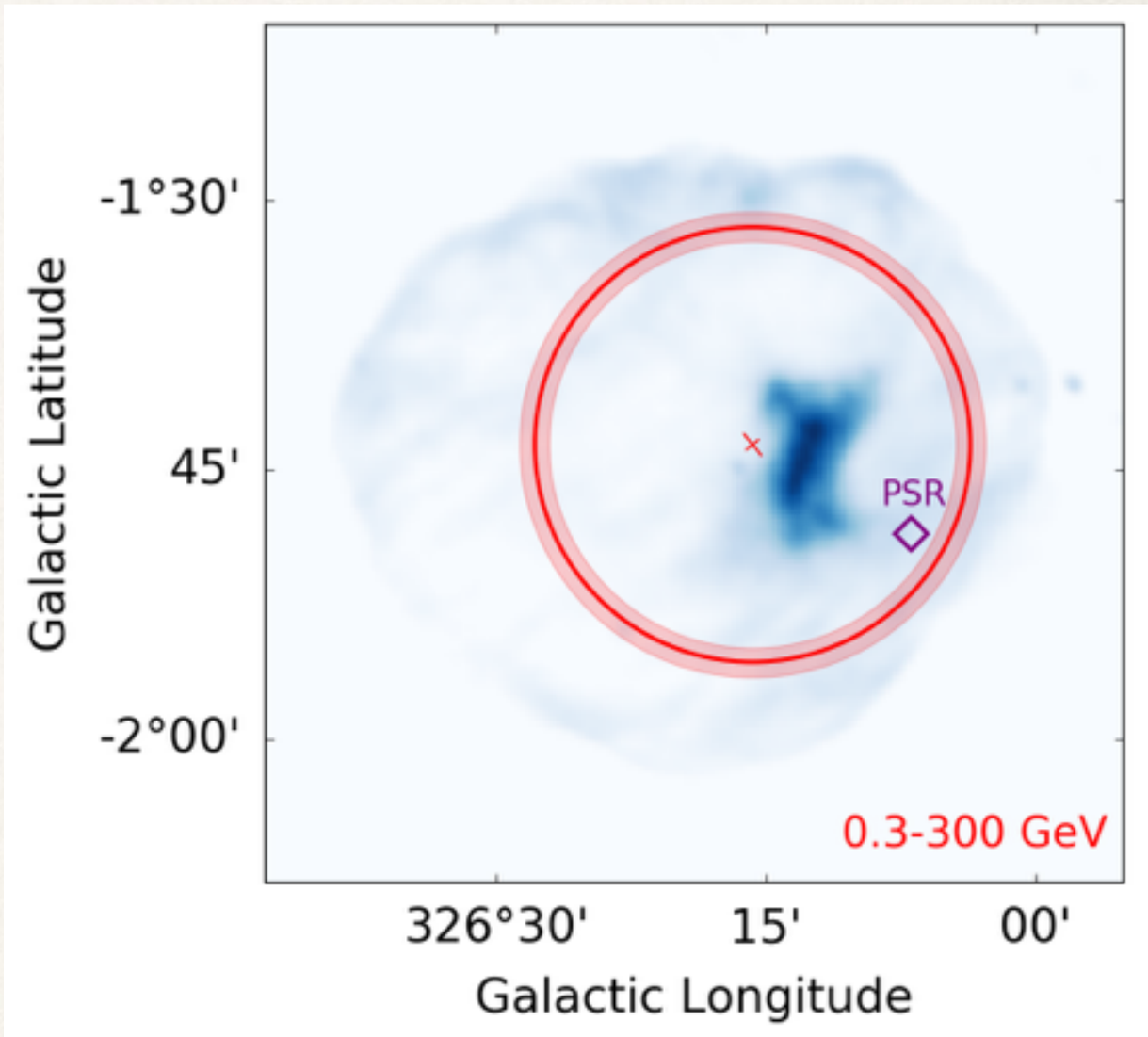


Best fitted disk (left) and Gaussian (right). Crosses: centroid uncertainties, solid circles: R68%, dashed circles: errors on size

# Energy-dependent morphology

## 2D symmetrical Gaussian fitted in 5 energy bands

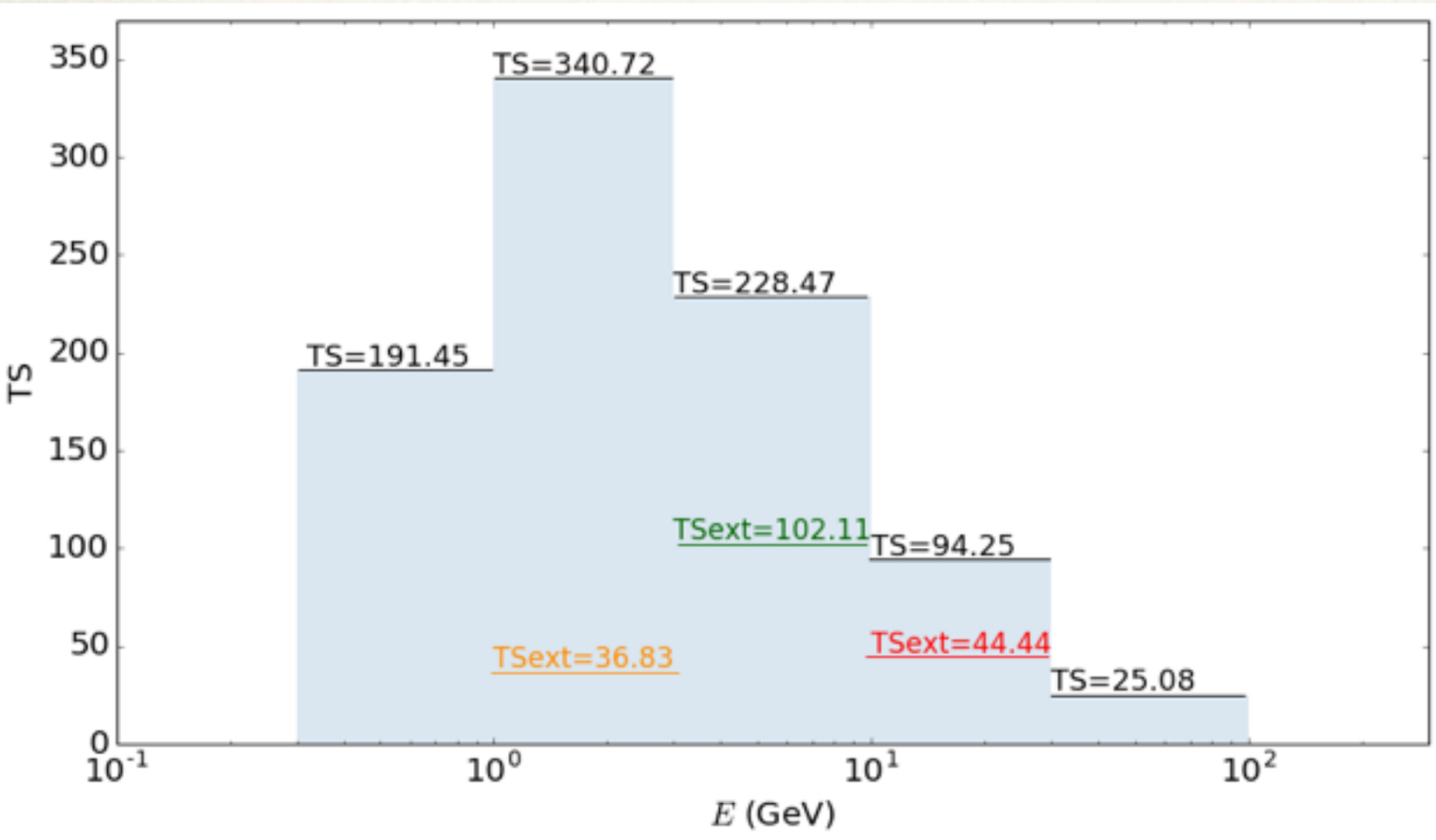


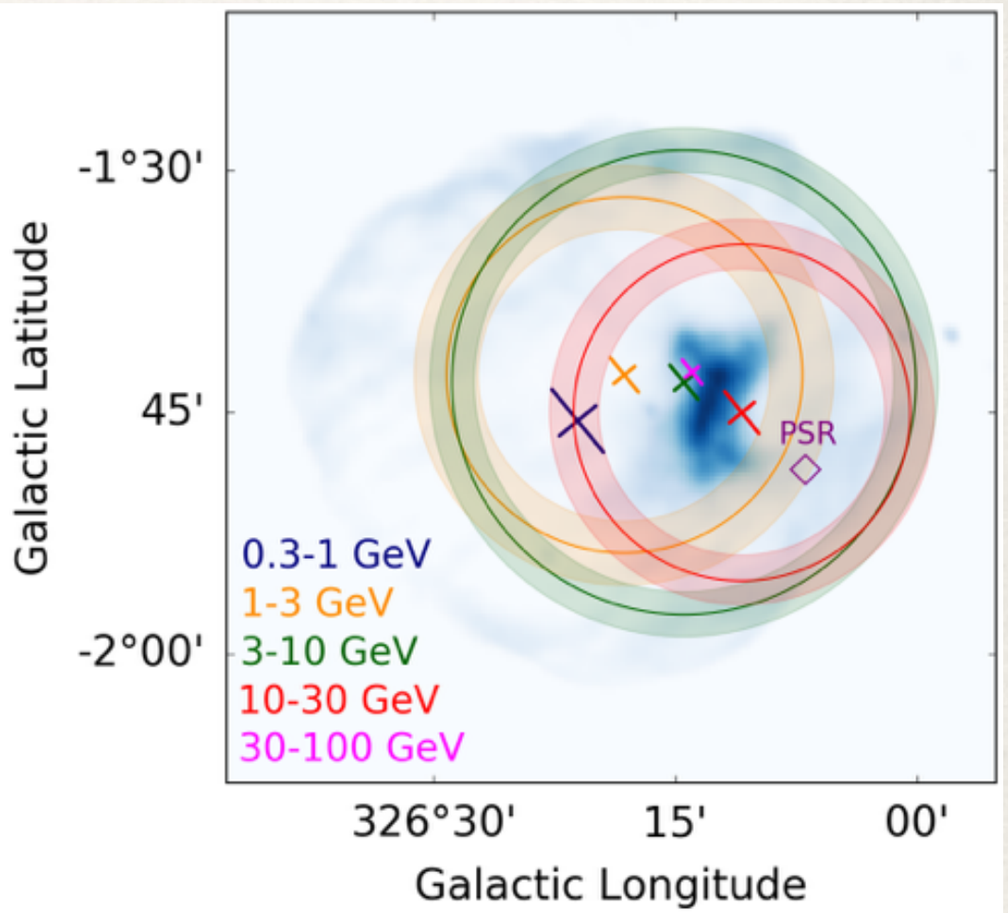


**Emission significantly extended from 1 GeV to 30 GeV**

**=> Clear trend toward the PWN at higher energies**

# MWL SED for the SNR

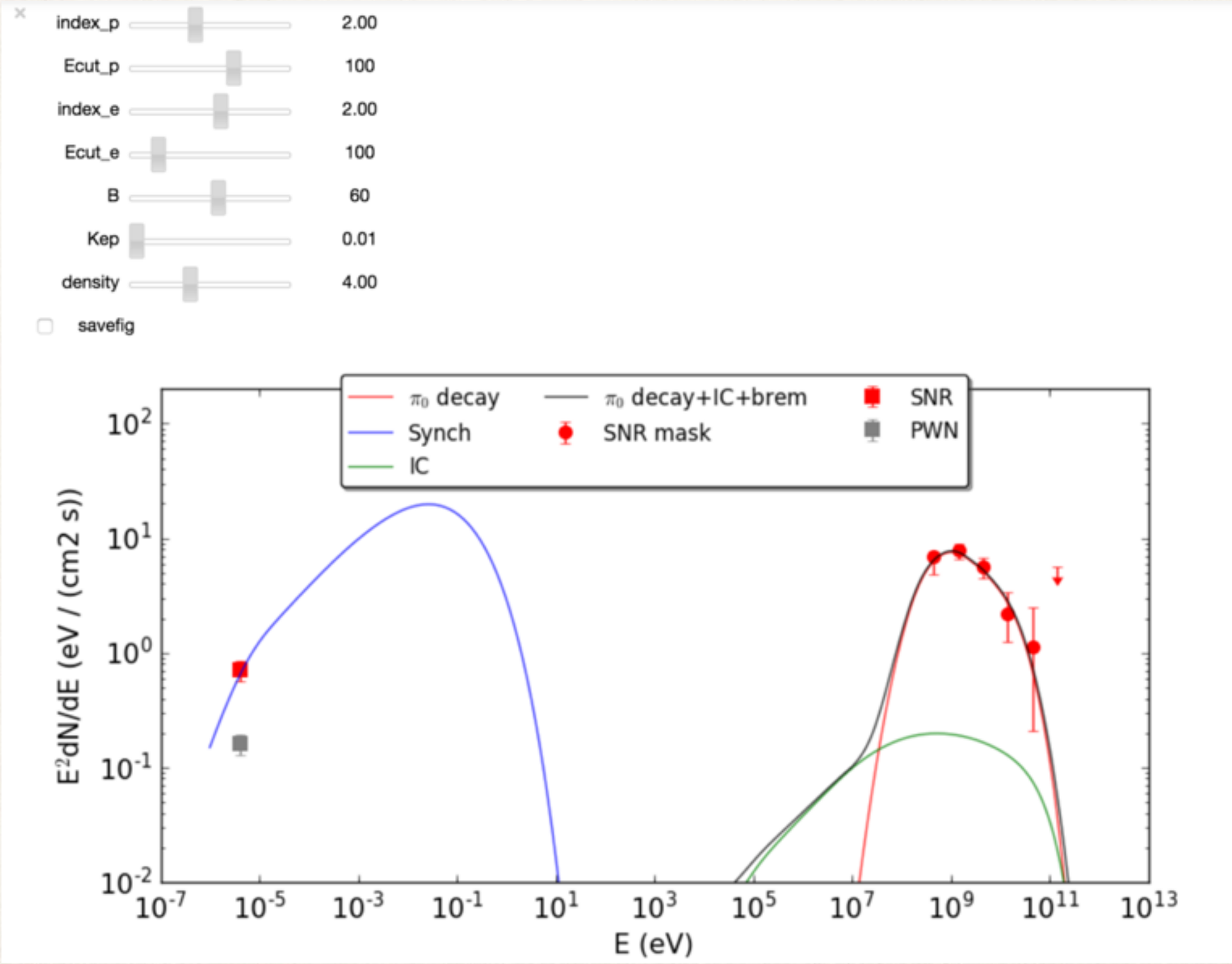

# Region Of Interest - PSF3 events

**From 300 MeV to 300 GeV**

**10 ° x 10 °**

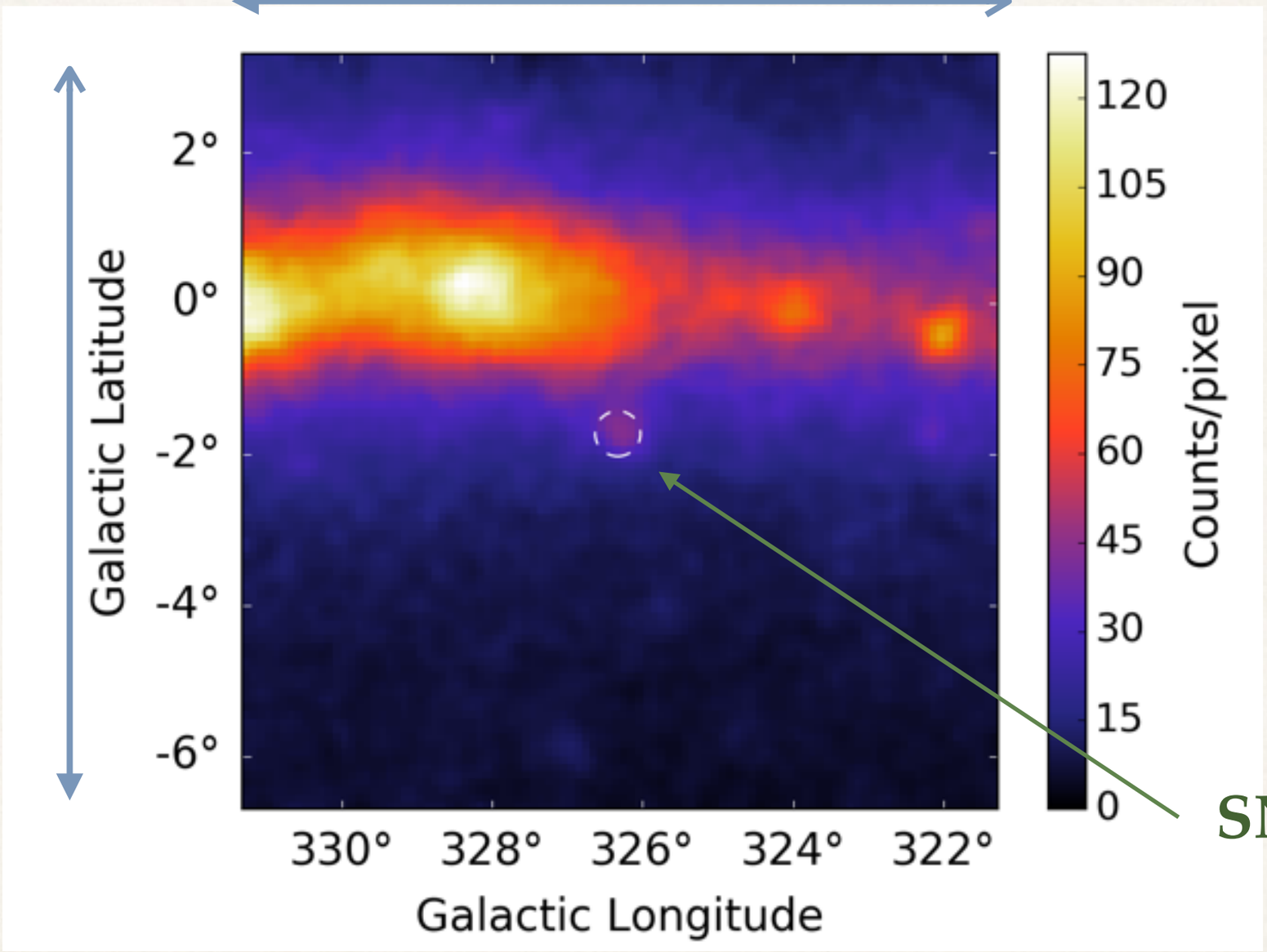


Still bright with PSF3 events

**SNR G326.3-1.8**

- 6.5 years of data
- binned analysis

# Morphological analysis

| | | | |
|---|---|---|---|
| *Point source* | 498.92 | 3 | — |
| *Disk* | 674.78 | 5 | — |
| *Disk + radio PWN[(b)]* | 688.11 | 7 | 13.32 |
| *Radio SNR[(a)]* | 660.09 | 2 | — |
| *Radio SNR[(a)] + radio PWN[(b)]* | 675.97 | 4 | 15.88 |
| *SNR mask[(c)]* | 663.18 | 2 | — |
| *SNR mask[(c)] + radio PWN[(b)]* | 689.42 | 4 | 26.24 |

**Residual TS map when only the SNR mask is included on the model (showing the contribution of the nebula):**

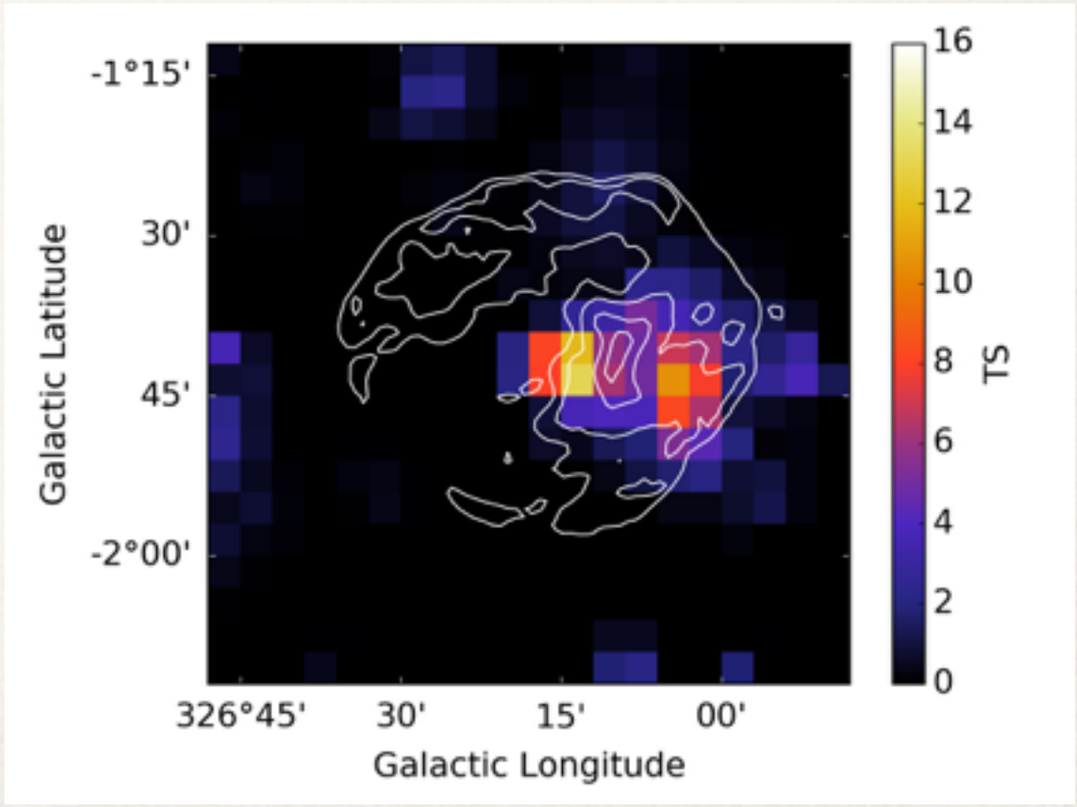

# TS map with radio PWN

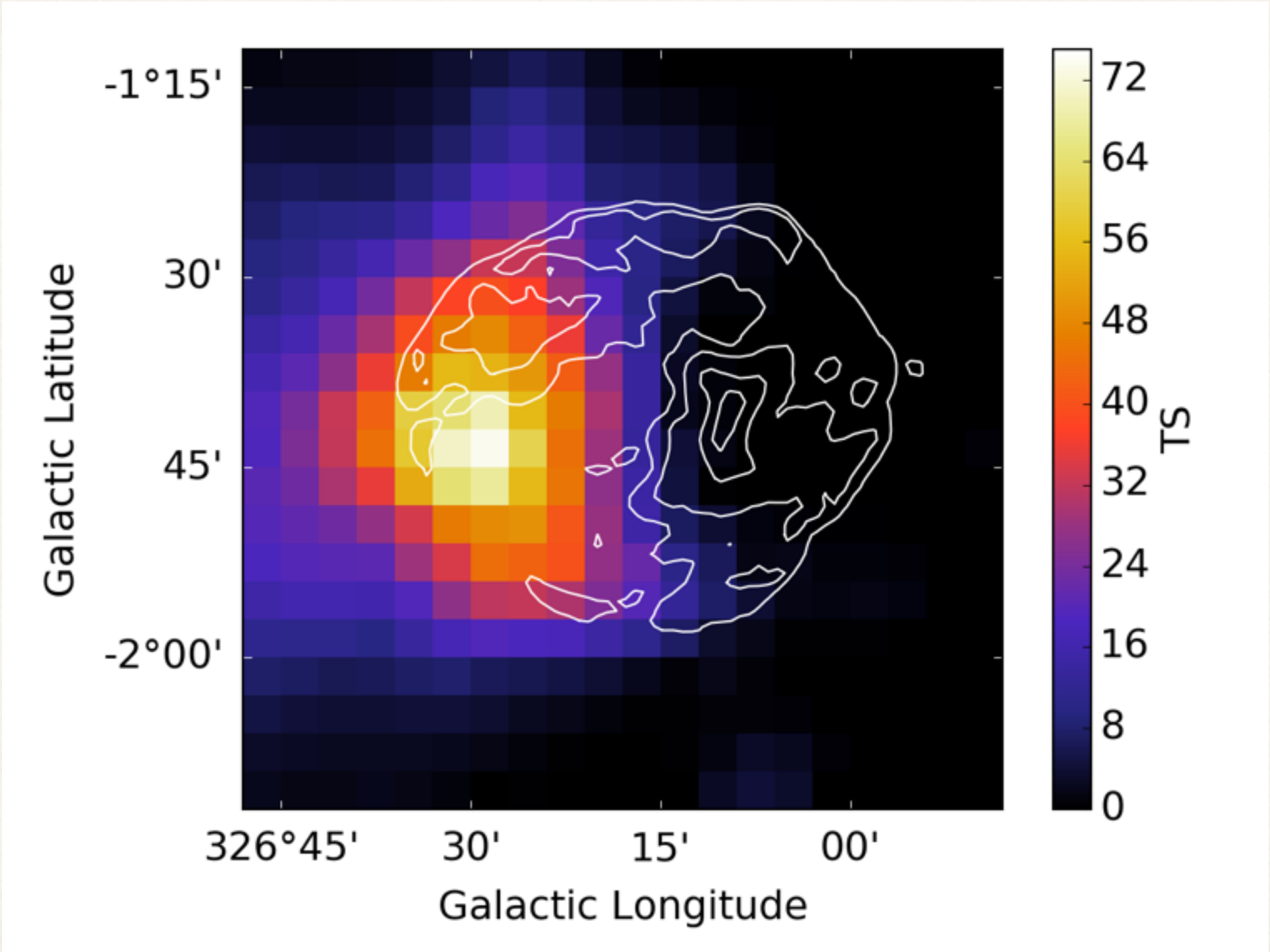

# Test Statistic maps per energy band

## 0.3 - 1 GeV

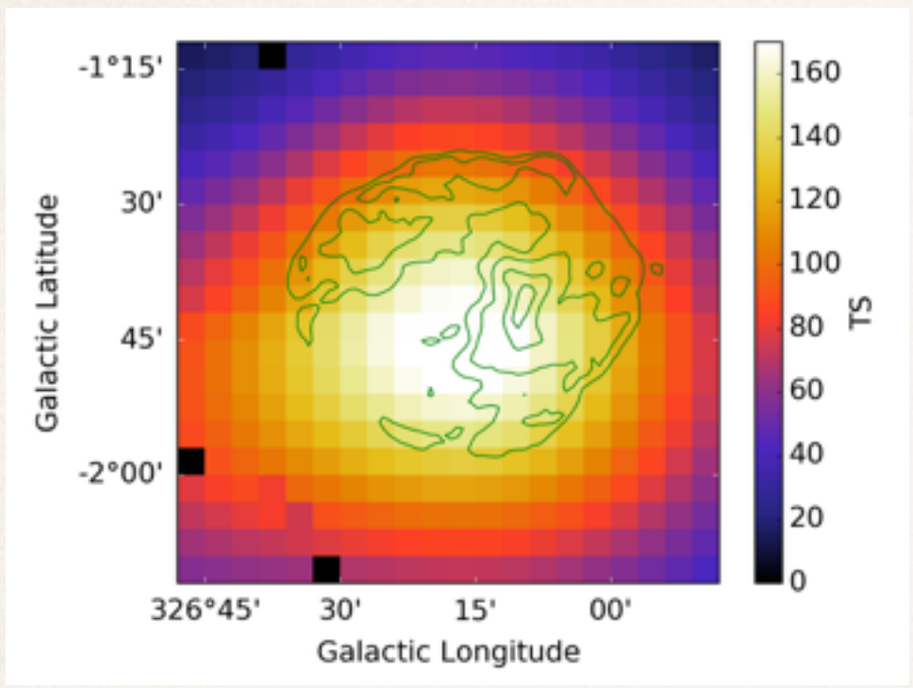


## 1 - 3 GeV

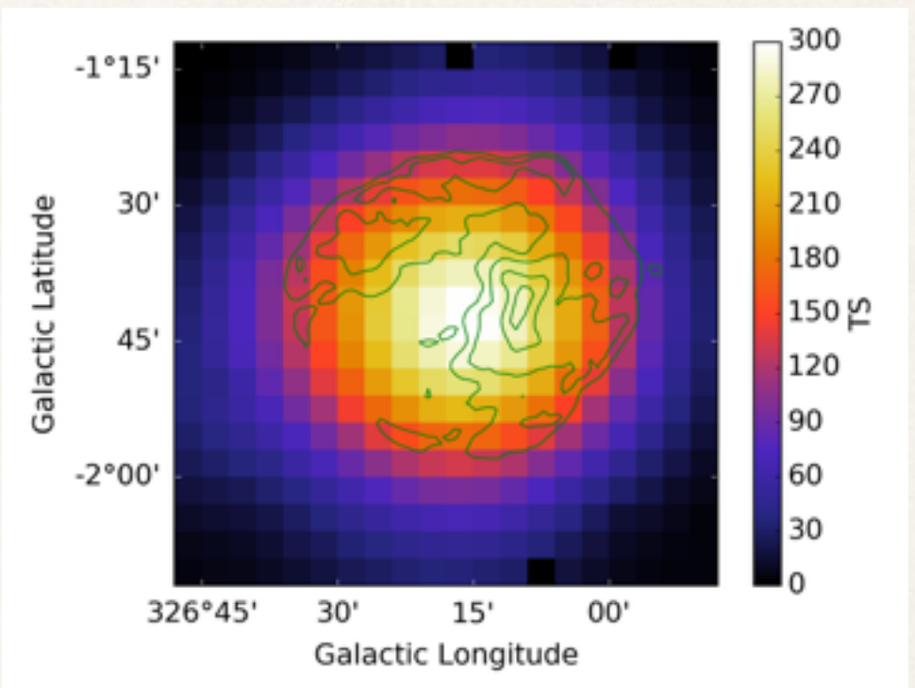


## 3 - 10 GeV

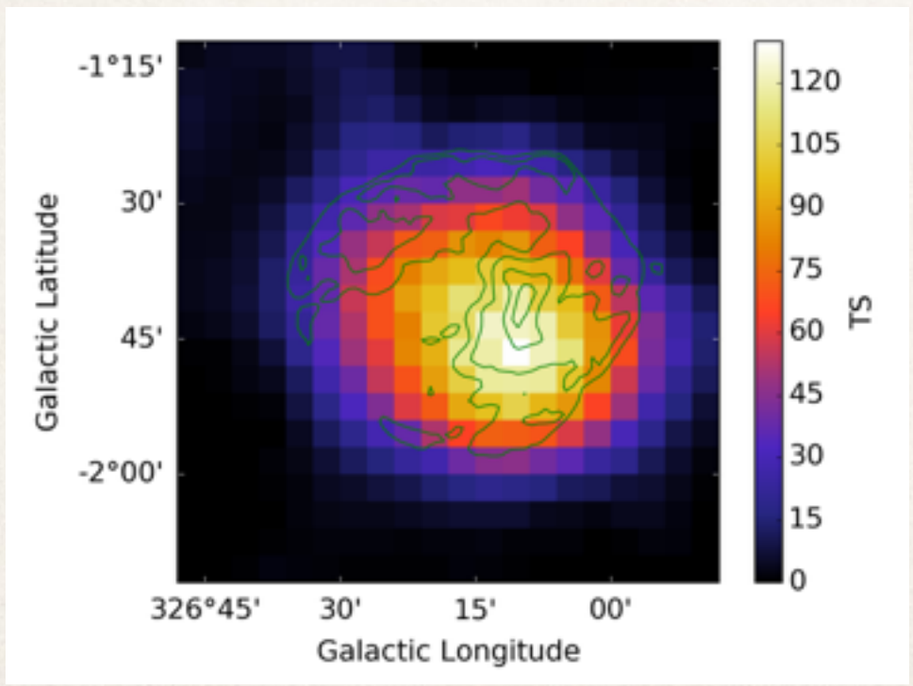


## 10 - 300 GeV

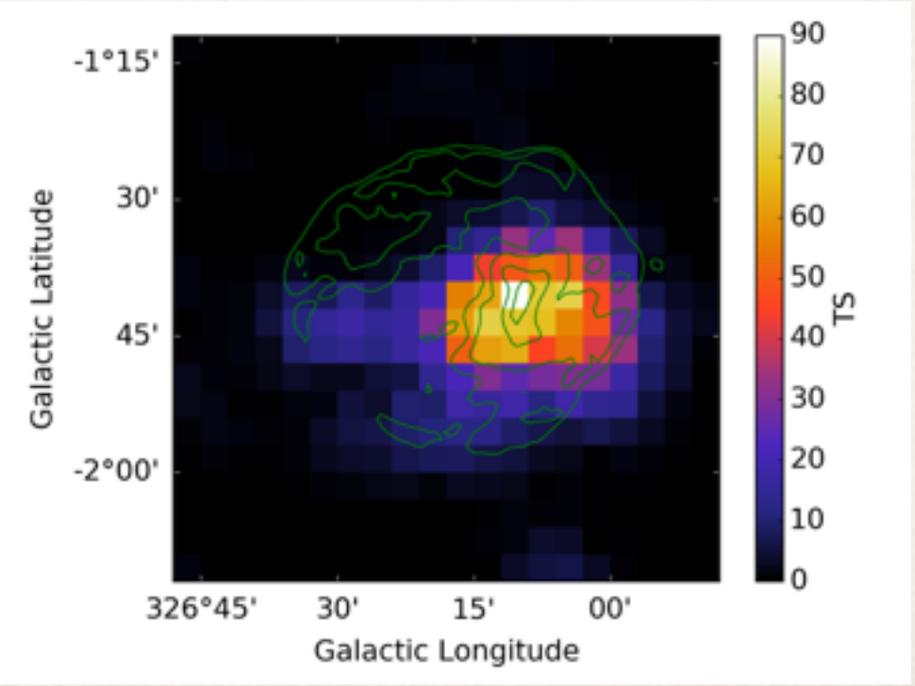

# Spectral analysis

**Fit from 300 MeV to 300 GeV:**

| | $\Gamma$ | $\Phi$ $(erg.cm^{-2}.s^{-1})$ |
|---|---|---|
| ***Disk*** | $2.07 \pm 0.04$ | $(2.70 \pm 0.15) \times 10^{-8}$ |
| ***PWN (radio)*** | $1.79 \pm 0.12$ | $(0.27 \pm 0.09) \times 10^{-8}$ |
| ***SNR (mask)*** | $2.17 \pm 0.06$ | $(2.29 \pm 0.24) \times 10^{-8}$ |

# Modeling the ROI

**Residual TS map:**

**10° x 10 °**
**pixelsize=0.2°**

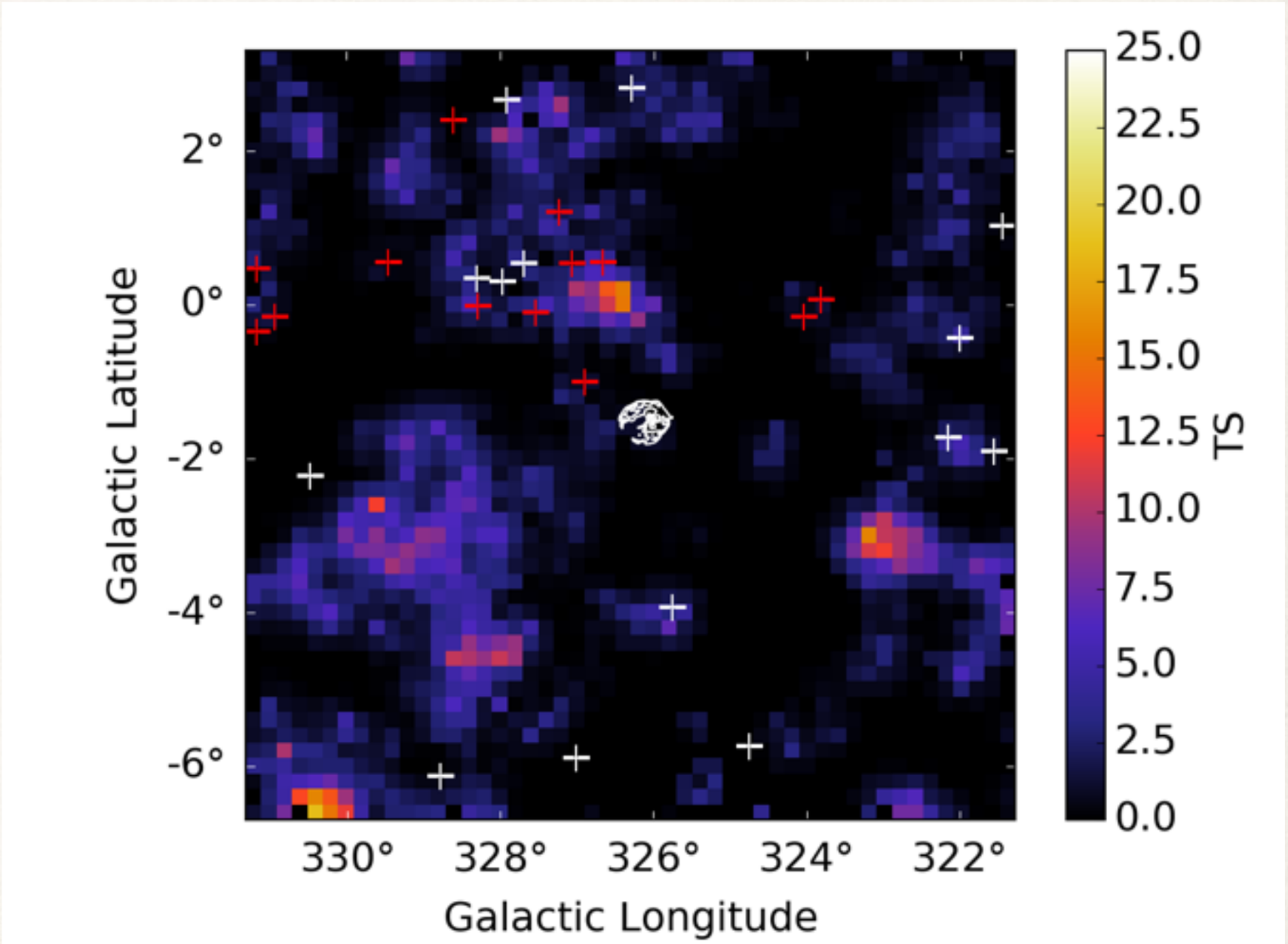


- 12 sources added (red crosses) + 3FGL sources
- the SNR is included

# Test Statistic

Count follow a Poisson statistics

Probability to obtain ni photon when the model predict lambda

$$P_i = \frac{\lambda_i^{n_i}}{n_i!} e^{-\lambda_i}$$

Total probability to obtain the data

$$L = \exp(-N_{pred}) \prod_i \frac{\lambda_i^{n_i}}{n_i!}$$

**log(L)=LL**

$$TS = 2 \times (LL_1 - LL_0)$$

$\Delta TS$ to compare two nested models

Chi2-law with n degrees of freedom

# Spectral energy distribution

## radio PWN + SNR ring:

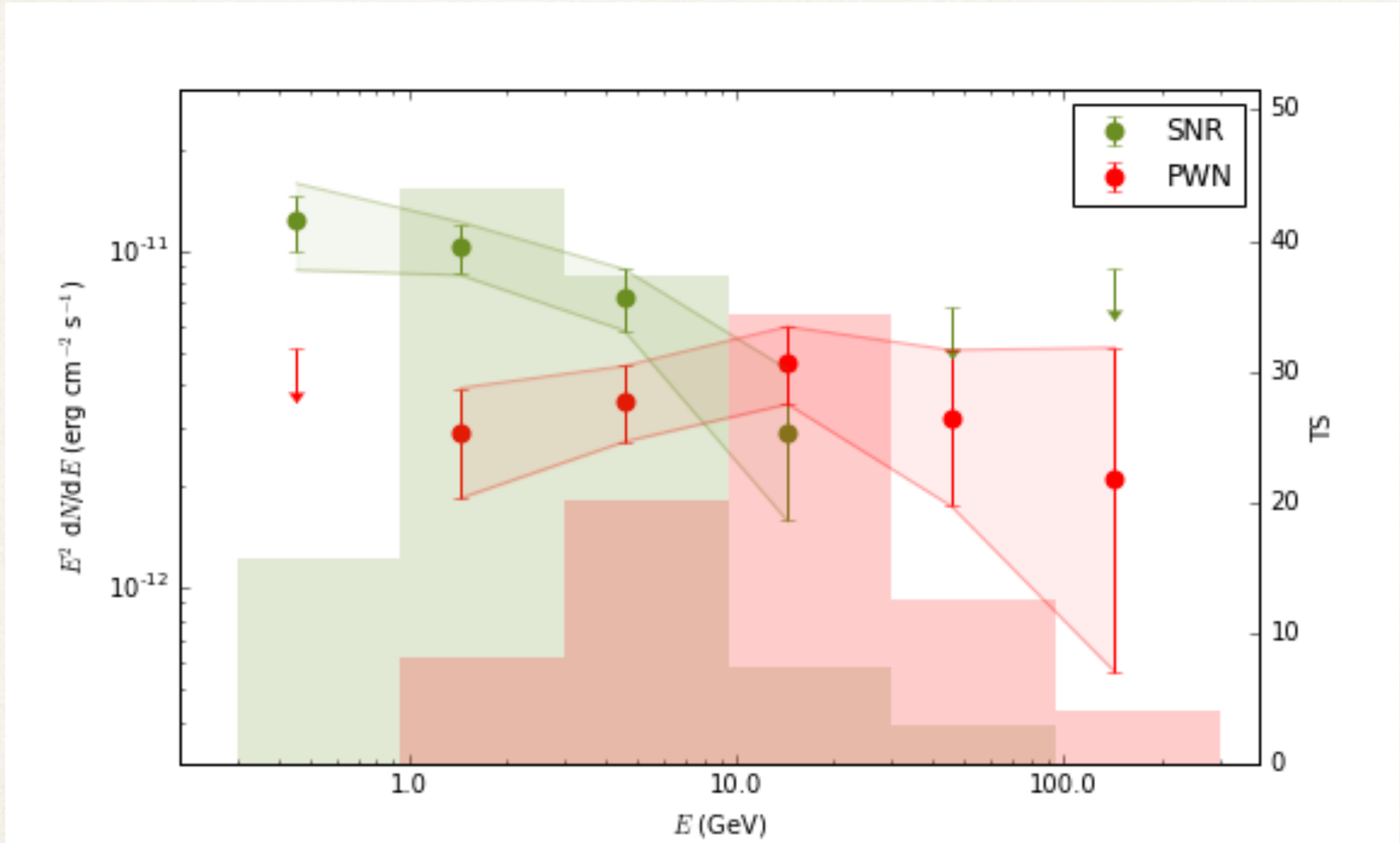


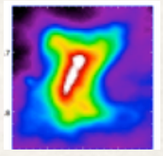

**Disk**

$\Gamma = 2.24 \pm 0.06$

**PWN**

$\Gamma = 1.83 \pm 0.09$

# Spectral energy distribution

## radio PWN + Disk:

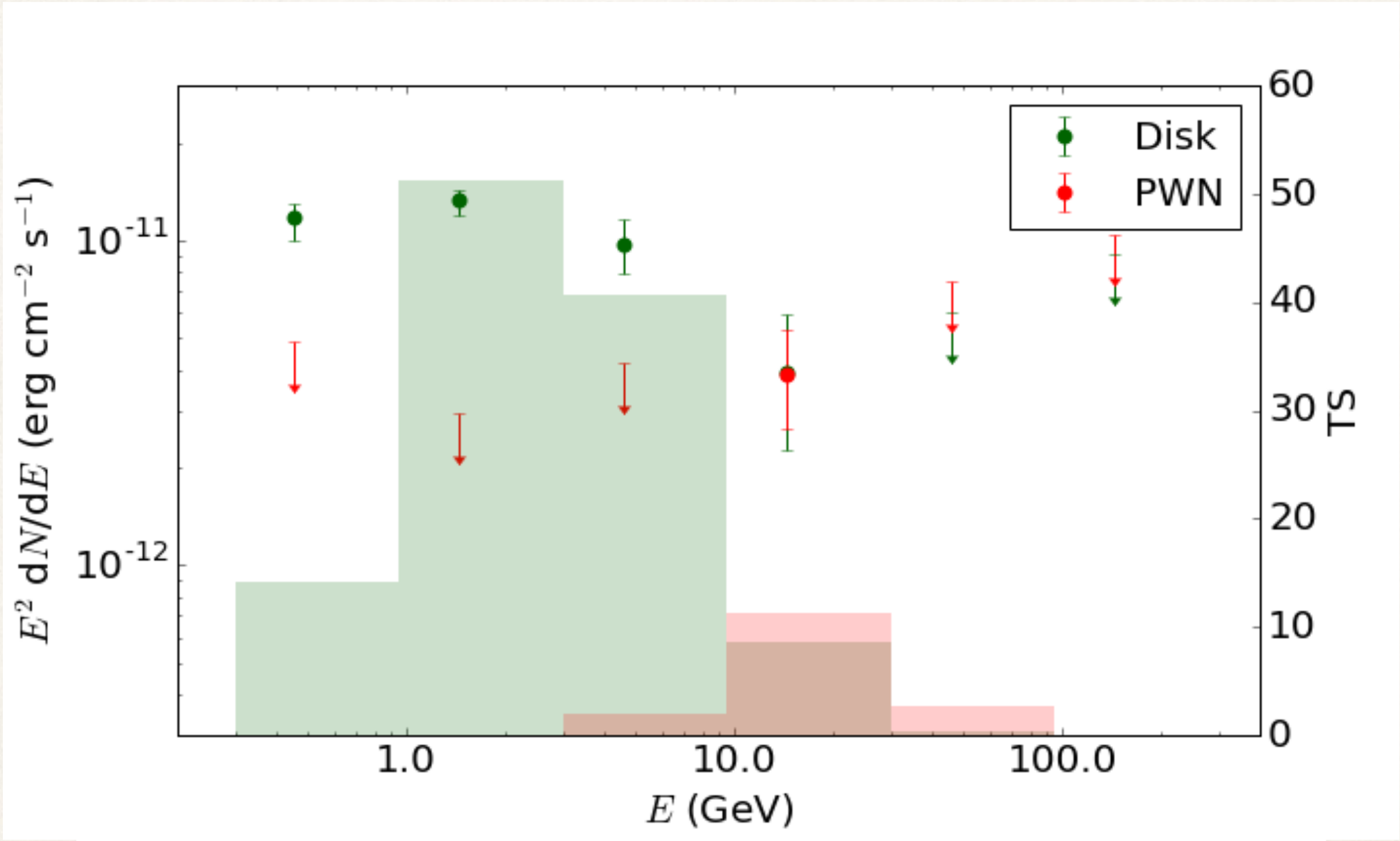


**Disk**

$\Gamma = 2.18 \pm 0.06$

**PWN**

$\Gamma = 1.75 \pm 0.15$

# Spectral energy distribution

## Disk:

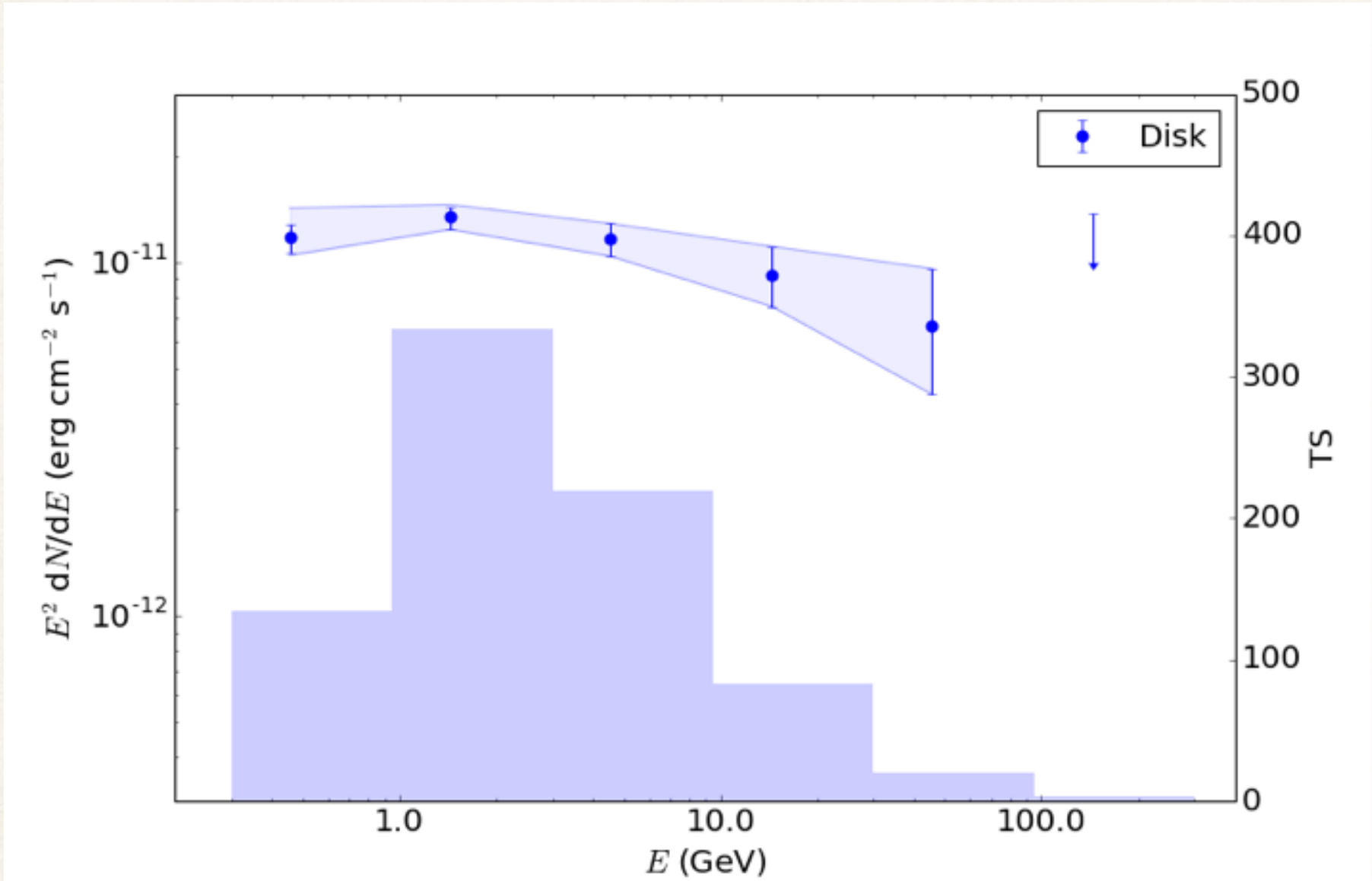


$\Gamma = 2.07 \pm 0.04$

# Parameters derived by Temim et al. 2013 - PWN

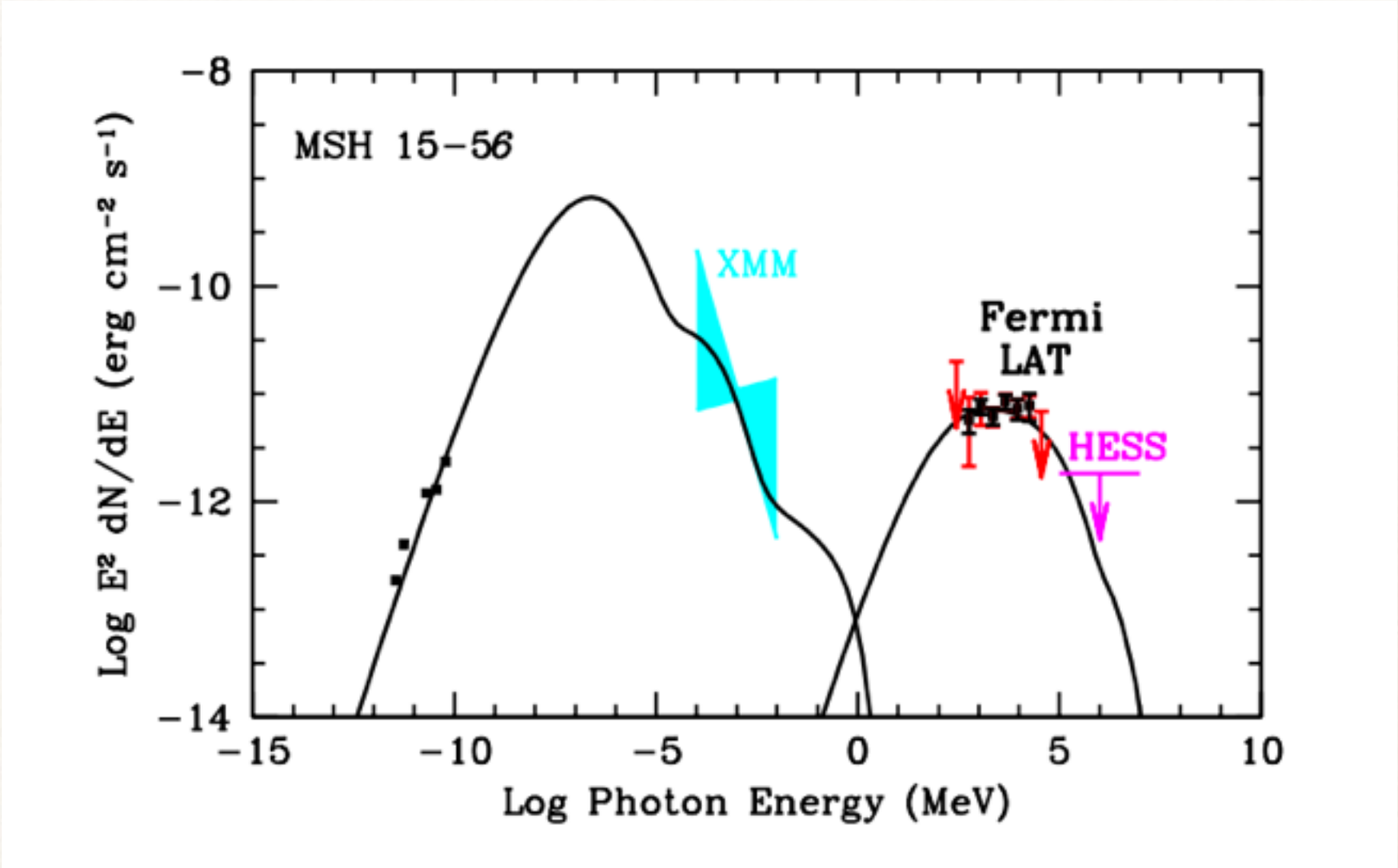

# Optical identification

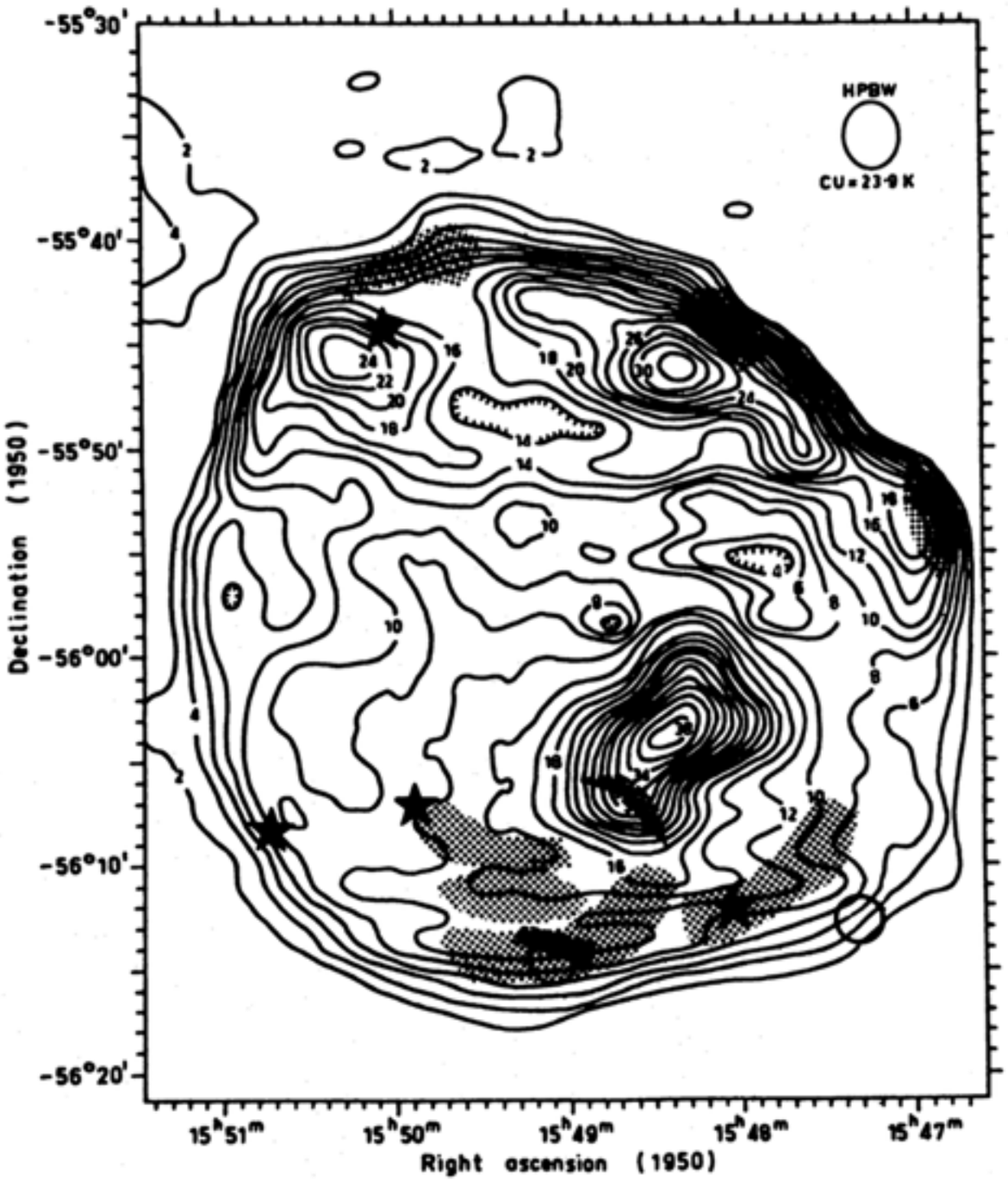


FIG. 2.—The distribution of Hα emission (*shaded*) is shown projected on the radio map by Clark, Green, and Caswell. The optical emission is seen to be associated with the outer shell of G326.3−1.8 and not with the polarized compact flat-spectrum component (Kes 25) contained within it. In the figure, asterisks mark the positions of the stars SAO 243056, 243092, 243093, and 243103. The positions of two new planetary nebulae are marked by circles.

**[Sydney Van Der Berg, 79]**

# Parameters derived by Temim et al. 2013

The radio emission is non-thermal, with a spectral index of $\alpha = 0.34$ for the non-thermal shell emission, where $S_\nu \propto \nu^{-\alpha}$, and 0.18 for the PWN component (Dickel et al. 2000). The PWN component is highly polarized, with a luminosity of $L_{10^7-10^{11}\,\mathrm{Hz}} \sim 5 \times 10^{34}\,\mathrm{erg\,s^{-1}}$, making the radio PWN in MSH 15–5*6* the third most luminous after the Crab and G328.4+0.2 (Dickel et al. 2000).